

SYSTEMATIC STUDY OF COATING SYSTEMS WITH TWO ROTATING ROLLS

F. BALZAROTTI and M. ROSEN

Grupo de Medios Porosos, Facultad de Ingenieria, Universidad de Buenos Aires, Argentina.

mrosen@fi.uba.ar

Abstract—The coating method called “Roll Coating” is one of the most widely used in industry and consists in the application of fluids through rotating rolls. In this work we examine the system of two cylinders in rotation. The aim of this presentation is to characterize this system of two cylinders for different ratio of velocities (s) and gap configurations, in order to build a phase diagram that identifies the resulting thickness for each set of operation parameter values. Resulting thicknesses were contrasted with classical models to test its validity limits. The classical models, which are based on the Theory of Lubrication, and their corresponding simplifying hypotheses, let us demonstrate the significant dependency of the outlet thicknesses with regard to the gap and the velocity ratio and the modified Capillary number β . When the amount of fluid dragged increases, an irregular V-shaped cross-site wave appears, repeated quasiperiodically down-web (Cascade effect), indicating the region of parameters in which the phenomenon is present.

Keywords—Roll coating, Seashore Phenomenon.

I. INTRODUCTION

The coating of surfaces with a liquid film is a process found in many applications. It is extensively used in the paint, paper, photography, magnetic tape and packaging industry to cover a large surface area with one or several uniform layers.

Although the products of these coating industries appear diversified, the same basic technologies are used to produce the required coatings and films.

There is a wide range of techniques to achieve the application of the fluid on a surface in a continuous way. The choice of the method depends on several factors. Among them, it is worth mentioning the nature of the surface to cover, the liquids rheology, the solvent that is used, the dry thickness required, the cover uniformity and the velocity of the covering process.

Usually, the layer of liquid should be thin, continuous, and uniform in thickness. However, instabilities of films are observed under certain operating conditions, which can only be analyzed by considering fluid dynamics problems associated with the coating process, as nonlinear events appear in the process.

“Roll Coating” is widely used in the industry and it consists in the application of the liquid through rotating rolls.

The flows between pairs of rotating rigid rolls have been extensively studied in some systems by means of

numerical methods (Samways, 1989; Meuthen, 1993; Evans *et al.*, 2004).

An important feature of roll coating is the presence of a fixed gap between the rolls, such fluid flow in the gap is the primary factor controlling the thickness and uniformity of the coated film.

Among numerous configurations, in this work, we focus on a system with two cylinders on direct rotation called “two-roll forward coater”.

Our goal is to characterize of this system for different spinning and gap configurations in order to build a diagram that identifies the resulting thickness for each set of parameter values in the experiment. Our results were compared with classical models to test its validity. In these systems, there may be two kinds of instabilities. At a certain velocity threshold, a hydrodynamic instability called “Ribbing instability” appears which extends smoothly across the liquid flow as a sinusoidal wave. On the other hand, when the amount of fluid dragged increases, a second instability may occur, an irregular V-shaped cross-stream wave, repeated quasiperiodically downstream (Cascade effect) appears. This last instability is particularly analyzed in this work. Once a flow field is found, its stability and disturbances must be evaluated and it is necessary to predict whether the flow will effectively displace air from the surface to be coated (Greener *et al.*, 1980; Ruschak, 1985).

In our system, a roll gets liquid continuously and a pump keeps the fluid level constant. By using more than one cylinder, it is possible to separate the supply from the application process, since the amount of liquid that can be pumped generally exceeds the required (Fig.1).

The specific design for each roll responds to operational issues. In Benjamin *et al.* (1995) a general review of different application systems is presented.

One of the main characteristics of the direct rotation fluid is the lack of dependence from the specific configuration of the rolls.

The pressure P exerted between the rolls is the key variable that controls the liquids transference in the process, while the differences in the rolls velocities adjust the applied final thickness.

Its worth mentioning that the applied pressure does not guarantee thickness control by itself because paint properties—as an example—may vary the flow across zones with an important deformation velocity due to the fluid’s rheology (Varela López *et al.*, 2002; Varela López and Rosen, 2002).

In our geometry (Fig.2), the axial length of the roll is approximately 10 times its diameter, and so the gener-

ated flux may be considered two dimensional except at the extremes. This feature, derived from geometry, is crucial to achieve uniformity in the covering thickness.

The liquid is forced to flow through the gap zone generating a pressure field on the surface (Varela Lopez *et al.*, 2003). On the exit zone (downstream), a part of the fluid is adhered to the covered surface, and the rest returns to the source (supplying) tray. As a consequence, a meniscus is produced where the two films split.

The systems behavior can be described by means of dimensionless numbers involving both the geometry and the fluids characteristics. The quotient between the gap and the rolls radius R is one of them, denoted as “geometric aspect relation”:

$$\Gamma = \text{gap}/R$$

On the other hand, in fluid dynamics systems with a free interface, capillary effects tend to be noticeable. A capillary number (Ca) is used to express the relation between the viscous forces and capillary forces, defined as:

$$\text{Ca} = \frac{\mu U}{T},$$

where μ is the fluids viscosity, T the surface tension and U the characteristic velocity. When the direction of the cylinder spinning is corotated, it is designated as “Forward Roll Coating”. Otherwise, if the spinning direction is counter-rotated, it will be “Reverse Roll Coating”. In general terms, the Reverse mode permits a greater range of thickness is more flexible than in the Forward mode.

Figure 1 shows a distribution as the one analyzed in this work.

II. EXPERIMENTAL SETUP

A laboratory model similar to those used in the industry was designed, made of two parallel rolls arranged horizontally (Fig. 2).

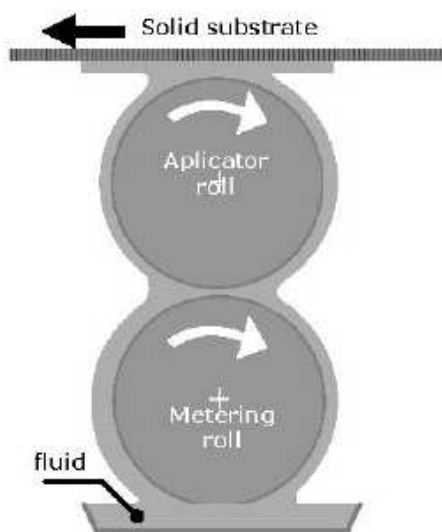


Figure 1. Two rolls system in Reverse mode.

The lower roll (Roll 2) is made of smooth stainless steel having a diameter of $75\text{mm} \pm 0.02\text{mm}$. It is in contact with the source tray and its function is to raise the

liquid (“Pick up roll”). Roll 1 (upper) has a steel core and an exterior coated with a deformable material (an elastomer, i.e. a polymer with the property of elasticity)¹. It is located parallel on top of roll 2 and separated by a very short but variable distance, compared to the diameters (gap). Roll 1 diameter has not the same geometric precision as roll 2: the former is $79.5\text{mm} \pm 0.5\text{mm}$. Both rolls are free to spin independently from each other through a set of bearings. The rolls are mechanically operated by two direct current motors, fed with independent voltage sources.

One or more velocity reducers can be added, depending on the required range of working velocity. The motor coupled to Roll 1 includes a closed loop system that controls the spinning velocity and keeps it constant within an error range of $\pm 0.5\text{rpm}$. The supplying source has an integrated display that indicates the spinning velocity measured by a tachometer.

The motor corresponding to Roll 2 is supplied with an ordinary voltage/current source which allows for a voltage variation ranging from 0 to 40V. Velocity is measured with an inductive sensor and a toothed wheel coupled to the spinning axis. The sensor is located close to the wheel to detect inductance variation between consecutive teeth. A second display shows the sensed information and translates it into rpm.

A vertical displacement system, consisting of two micrometric screws located on the sides of roll 2 on top of each bearing, allows for the calibration of the gap at a step of 0.5mm and independent movements from each other.

The gap is defined as positive because the operating distance between the rolls admits only a minor deformation of the flexible roll. Consequently, the outcome is as expected in the case of rigid gaps (Carvalho and Scriven, 1977).

III. CLASSICAL TREATMENT

The classical models (Coyle, 1984) of the flow generated between two cylinders rotating in the corotation direction (Forward mode), let the coating thickness dependence be obtained from the cylinder velocity and the gap.

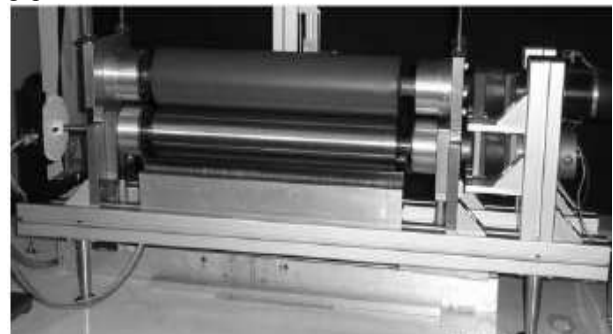


Figure 2. Laboratory model in detail.

Considering two rotating cylinders radii R_1 and R_2 , with tangential velocities of U_1 and U_2 respectively, separated by a gap H_0 , and applying the lubrication condition, it is possible to obtain an expression for the output

¹ It was made by Argentine steel company SIDERAR.

h_1^∞ y h_2^∞ thicknesses (Fig. 3)

Assuming a parabolic approximation for the expression of the convergent/divergent channel, it is possible to obtain an expression for the gap:

$$h(x) = H_0 + x^2 / R.$$

where the applied simplifications do not affect the final results, and the error is lower than 1.5% for the operating range. (Balzarotti, 2007).

Assuming that the cylinder axis length is greater than the L_y (gap) and L_{xz} scales (typical scales) the flow can be taken to be approximately two dimensional, where pressure would be a constant in the z direction. The flow in the gap region is nearly rectilinear and the governing Navier-Stokes equations are valid, as it is the lubrication theory at least far enough from the meniscus upstream and downstream. In addition, assuming complete adherence (or “total wetting”) of the fluid on the cylinder surface and neglecting the vertical component of tangential velocity, one can obtain:

$$\frac{\partial p}{\partial x} = \frac{6\mu}{h(x)^3} [(U_1 + U_2)h(x) - 2Q].$$

Notice that this approximation is only valid for a small curvature, i.e. $\partial h/\partial x \ll 1$. This expression describes the pressure gradient in the gap as a function of the x coordinate and Q (flow). Therefore, the boundary conditions depend on the flow behavior in the meniscus zone.

There are two possible analytical approaches (Savage, 1982):

- Separation Model.
- Reynolds Model.

In the first model, the role of the capillary pressure in the meniscus is taken into account and it is obtained an expression of the thickness reached in terms of the modified capillary number and the velocity ratio (Savage, 1982).

Thicknesses are defined as a function of the dimensionless variables involved (Fig. 3):

$$\lambda_1 = h_1^\infty / H_0 \quad \text{and} \quad \lambda_2 = h_2^\infty / H_0$$

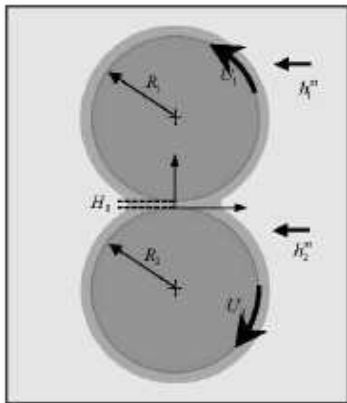


Figure 3. Detail of the geometrical characteristic.

As a function of which the pressure gradient can be expressed and where the modified Capillary number is introduced:

$$\beta = \frac{T}{\mu U} \left(\frac{H_0}{R} \right)$$

where $U = (U_1 + U_2)/2$, β is connected to the dimensionless parameters described in Section I: $\beta = \Gamma^{1/2} / Ca$, $s = U_1 / U_2$ is also defined as the velocity of both cylinders. With these approximations λ_1 and λ_2 thicknesses are equal for $s=1$, i.e. when tangential velocities are equal. This is due to symmetry of the configuration of cylinder tangential velocities. Besides, this approach offers greater sensitivity with s than with β .

Reynolds Model postulates that at some points in the flows both the pressure and its gradient vanish. Therefore, with $\beta \ll 1$ values (high pressures), the capillary effects are negligible and this model usually predicts higher pressures than those of the Separation model. The meniscus retreats, eliminating the depression zone.

Under equal operating conditions, the Separation Model predicts greater thicknesses and lower pressures compared to the Reynolds Model.

The introduced models offer an application range in which the Separation model is valid for $\beta > T/H_0 (\rho_{atm})^{-1}$ and Reynolds Model for $\beta < T/H_0 (\rho_{atm})^{-1}$.

IV. THICKNESSES

In order to measure the fluid layer thickness on the upper roll (h_1^∞), an optical method of image acquisition and digitalization was used. The acquisition was made with a CCD camera horizontally arranged, so that the lens faces the upper roll perpendicularly. The lighting system consists of a white light located behind the rolls with an acrylic plate (diffuser) in front of it. The latter ensures light homogeneity.

A relation of 700 pixels every 9mm was used, which implies a scale factor of 0.0128mm/pixel. This value in turn represents an upper bound for the measurement error.

A. Velocity Relation

Figure 4 presents the results obtained for h_1^∞ with U_2 as parameter and for different U_1 values with a fixed gap of 0.7mm.

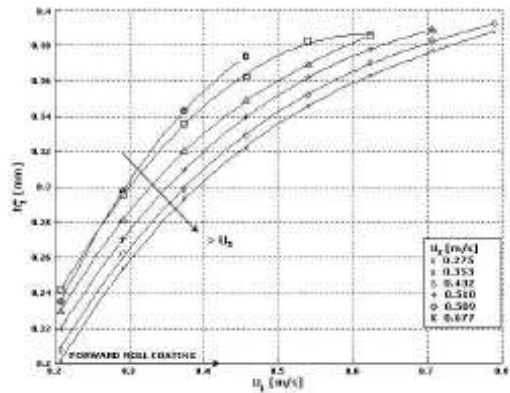


Figure 4: h_1^∞ thickness (gap = 0.7mm) measured in “Forward roll coating” mode ($U_1 > 0$).

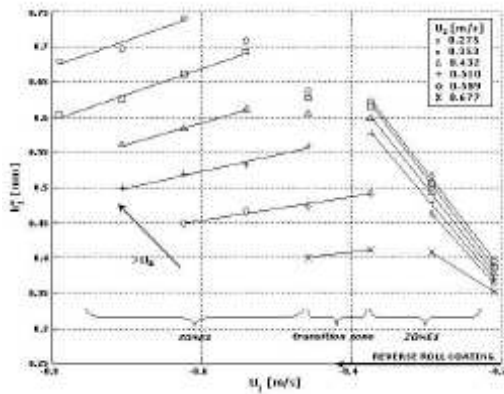


Figure 5: h_1^∞ thickness (gap = 0.7mm) measured in “Reverse mode”.

Measurements were made in different zones of the upper roll surface and then they were averaged, it was possible because under equal velocity combination, the deviation of the results came up to be less than 5%.

It can be clearly observed in Figures 4 and 5, that there is a very different behavior in the system performance depending on the operating mode used.

Forward Mode: In this mode, h_1^∞ thickness grows when U_1 increases and decreases when U_2 increases. In all cases, its value was within 0.2 and 0.4 mm. The dotted lines indicate a cubic adjustment of the different U_2 constant velocity curves.

Reverse Mode: It is possible to determine two zones with opposite behaviors: for U_1 values, in the range of 0.2-0.4m/s, Zone 1 can be observed, where the h_1^∞ thickness increases linearly for all the values of U_2 . This tendency reaches its maximum value and then there is a Zone 2, in which h_1^∞ decreases also linearly with U_1 . In this second zone, decreasing curves are roughly parallel among them and closer to each other than those in Zone 1. Contrary to the Forward mode, thickness grows when U_2 increases. Therefore, in the Reverse mode there is discontinuity in thickness variation.

Between Zone 1 (increase) and Zone 2 (decrease), there is a middle or transition region. In this velocity range, there appear sinusoidal patterns on the rolls. This behavior, which will be described in Section I, corresponds to the “Cascade Effect” (also called “Seashore Phenomenon”), in which flow is no longer two dimensional, but appears as a sinusoidal pattern on each roll (Gaskell and Savage, 1997).

B. Gap Influence

Figures 6 and 7 present the results for both modes. In the Reverse Roll Coating mode, the intermediate region between two different behaviors appears again.

Forward Mode: The range of the obtained thicknesses is outstandingly modified depending on the calibrated gap, thus achieving lesser thicknesses for lower gap values.

Reverse Mode: Contrary to the Forward mode, thicknesses of the three values of the calibrated gap have similar magnitudes among them.

However, in Zone 2, thicknesses decrease with higher slope when the gap diminishes.

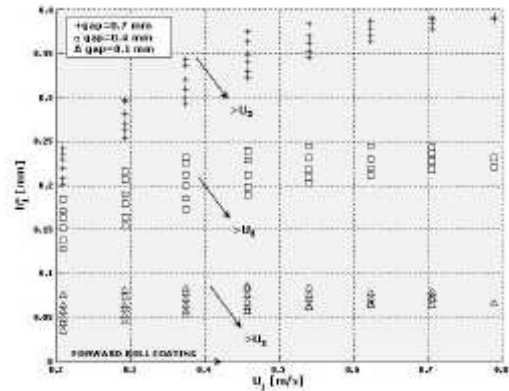


Figure 6. Thickness h_1^∞ gap influence in “Forward mode” (0.27m/s< U_2 <0.67m/s).

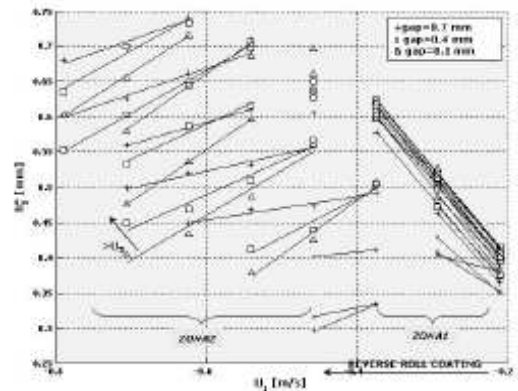


Figure 7. Thickness h_1^∞ . Dotted lines join the obtained results for the same gap.

Table 1. Obtained range of thicknesses according to the operating mode and calibrated gap.

Gap (mm)	h_1^∞ Forward Mode	h_1^∞ Reverse Mode
0.7	200-400	400-750
0.4	125-250	350-750
0.1	35-80	300-750

As a summary, Table 1 indicates the different values of h_1^∞ that were obtained.

C. Limits of classical models for the Forward Roll Coating case.

Figure 8 was obtained by representing the experimental system variables U_1, U_2, H_0 y h_1^∞ with the domain of the dimensionless variables defined in Section III. In Fig. 8 we contrast the Separation Model with our experimental results corresponding to $0.1 < \beta < 0.8$.

In this figure, it can be observed that the model (associated to the lubrication approximation) predicts a thickness λ_1 slightly greater to the one obtained in practice. However, the increasing tendency of λ_1 with s agrees in all cases.

As it is expected, the smaller the gap is, the more concordance there is between the experimental results and the predicted ones. This behavior is compatible with the hypotheses made to apply the approximations of Lubrication, where the relation of scales L_y/L_{xz} was required to be of the order of 10^{-3} . A natural scale for L_y is the gap, whereas L_{xz} is $\sqrt{H_0 R}$.

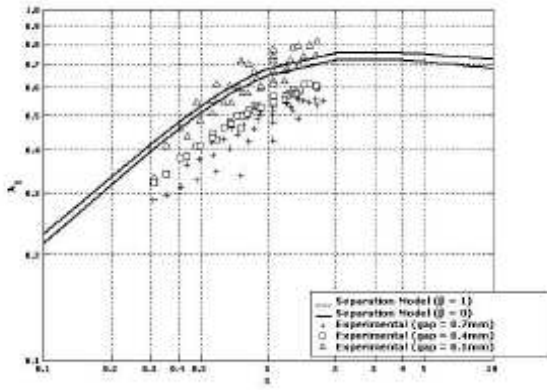


Figure 8. Dimensionless thickness λ_1 Separation model vs. experimental results (Forward mode).

Table 2 Scales relation according to calibrated gap.

Gap (mm)	$L_y / L_{xz} = \sqrt{H_0 / R} = \sqrt{\Gamma}$
0.7	0.13
0.4	0.10
0.1	0.05

Table 2 indicates the different scale relations for each calibrated gap.

As it can be observed, the obtained relation of scales do not comply with the approximations of Lubrication, where Γ should be of the order of 10^{-6} , something difficult to achieve with our experimental system.

D. Unstable behavior

Some hydrodynamic instability in Reverse mode only (Coyle *et al.*, 1990; Alonso-Romero, 2000) was observed under certain operation circumstances, when measuring the thickness of the fluid layer on the upper roll.

In Fig. 9 it can be observed that the phenomenon presents different patterns on each roll; the pattern is sinusoidal in the upper roll and generates V-shaped lines in the lower roll

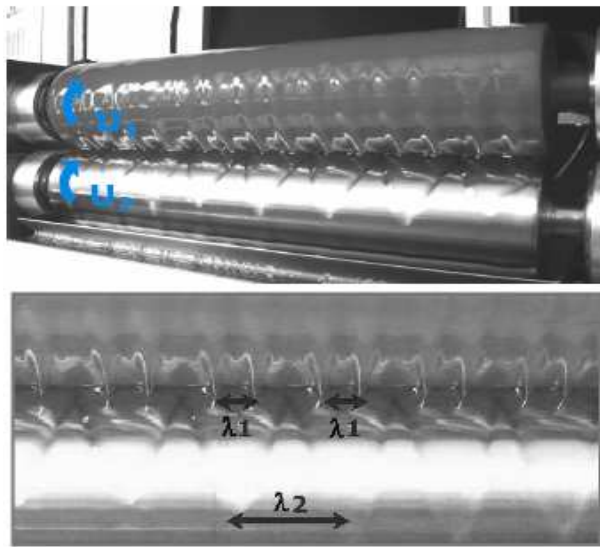


Figure 9. Hydrodynamic instability observed during the measuring of the thickness in the upper roll ($U_1=0.5m/s$, $U_2=0.6m/s$)

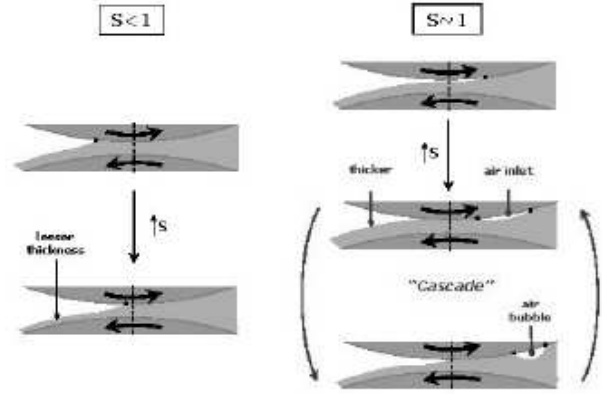


Figure 10. Cascade or seashore pattern running across the web produced by trapping of air in the meniscus when it is pulled through the gap by a high metering roll velocity (Alonso Romero, 2000).

Table 3 -Wavelength according to spinning velocity

U_1 (m/s)	U_2 (m/s)	λ (mm)
0.43	0.64	$\lambda_1 = 17$
0.47	0.64	$\lambda_1 = 15$
0.50	0.64	$\lambda_1 = 19 \quad \lambda_2 = 45$
0.53	0.64	$\lambda_1 = 19 \quad \lambda_2 = 36$
0.57	0.64	λ_2 non defined
0.61	0.64	λ disappears

When the velocity of the upper roll was further increased, the unstable pattern would disappear completely and the system would return to the bi dimensional configuration.

The phenomenon is described in Fig. 10, the evolution of the pattern for velocity increases of the upper roll (U_1) is characterized and the velocity of the lower roll is kept constant (U_2).

During the development of the instability formation process, the respective wavelengths and the relation of velocity that led to it were measured (Table 3). A slight displacement of the threshold velocity was detected according to whether U_2 was increased or decreased for a fixed value of U_1 which indicates a certain hysteresis of the triggering process (Coyle, 1984; Alonso Romero, 2000).

The results are repetitive despite the narrow margin of the velocity range in which this behavior is observed. The values reached by h_1^∞ just before the instability appeared can be explained with a simple model proposed by Moffat (1977), who analyzed the behavior of a viscous liquid layer on the external surface of a rotating cylinder. Starting from Navier-Stokes equations and their corresponding simplifying hypotheses (where the inertia and capillary effects are neglected), one can find an analytical solution for the tangential component of the velocity in the viscous layer. Moffat (1977) also obtains the following relation for the thickness:

$$h_{sup} < \frac{2}{3} \left(\frac{Uv}{g} \right)^{1/2}$$

that matches our experimental measure since we

obtained a value of 0.68 mm just before the instability, while 0.72 mm was expected with Moffat's model. This result falls within the experimental errors.

V. CONCLUSIONS

Experimental equipment that allowed modeling the Roll Coating process was built and characterized. In this work, the covering process with rolls was studied and the involved variables were analyzed. A deeper knowledge of the process dynamics was gained through the tests to improve the industrial model approximation and to control the covering thickness of the specific operational conditions.

The examined classical models, which start from the Lubrication Theory and their simplifying hypotheses, allowed us to establish the strong dependency of the outlet thicknesses with respect to the gap and the velocity relation (s), but not regarding the modified capillary number (β).

The Separation model is the one that fits our own experimental results, even if the predicted values are slightly higher than those obtained. Remember that, under the same operational conditions, this model predicted thickness values that were higher than those in the Reynolds model. As we expected, the thicknesses in Forward mode turned out to be highly dependent on the gap. This work showed that the laboratory model allows for reproducible results that can be analyzed with conventional tools, despite the fact that it does not strictly comply with the Lubrication hypotheses.

For the first time, when the "cascade" instability was examined, a narrow range of velocity could be established, so that instead of a characteristic behavior of the non-linear systems, which present an evolution towards a chaotic state (Rosen and Vazquez, 2007), a region could be defined, where a stable situation can be reached by modifying one of the control parameters. This phenomenon is a complex one (Ruschak, 1985; Decre *et al.*, 1995; Benkeira, 2002), involving both macroscopic flow effects and microscopic events at a dynamic wetting line.

REFERENCES

- Alonso Romero, S., *Metering film hydrodynamics in film coating*, PhD Thesis, Université de Montréal, Canada (2000).
- Benkeira, H., "Dynamic wetting in metering and pre-metered forward roll coating," *Chemical Engineering Science*, **57**, 3025-3032 (2002).
- Balzarotti, F., *Dinámica del proceso recubrimiento de chapas con rodillos*, Tesis de Ingeniería Mecánica, UBA, Argentina (2007).
- Benjamin, D.F., T.J. Anderson and L.E. Scriven, "Multiple Roll systems: Steady-State Operation," *AIChE J.*, **41**, 1045-1049 (1995).
- Carvalho, M.S. and L.E. Scriven, "Deformable roll coating flows: steady state and linear perturbation analysis," *J. Fluid Mech.*, **339**, 143-172 (1977).
- Coyle, D.J., *The fluid mechanics of roll coating: steady flows, stability, and rheology*, PhD Thesis, University of Minnesota, USA (1984).
- Coyle, D.J., C.W. Macosko and L.E. Scriven, "Stability of symmetric film-splitting between counter-rotating cylinders," *J. Fluid Mech.*, **216**, 437-458 (1990).
- Decre, M., E. Gailly and J.M. Buchlin, "Meniscus shape experiments in forward roll coating," *Phys. Fluids*, **7**, 458-467 (1995).
- Evans, P.L., L.W. Schwartz and R.V. Roy, "Steady and unsteady solutions for coating flow on a rotating horizontal cylinder: Two-dimensional theoretical and numerical modeling," *Phys. Fluids*, **16**, 2742-2756 (2004).
- Gaskell, P.H. and M.D. Savage, "Thin liquid films and coating processes," *von Karman Institute for Fluid Dynamics*, Lecture Series (1997).
- Greener, J., T. Sullivan, B. Turner and S. Middleman, "Ribbing instability of a two-roll coater: newtonian fluids," *Chem. Eng. Commun.*, **5**, 73-83 (1980).
- Meuthen, B., "Coil Coating in Germany," *Met. Plant and Tech. Int.*, **2**, 102-107 (1993).
- Moffat, H.K., "Behaviour of a viscous film on the outer surface of a rotating cylinder," *Journal de Mécanique*, **16**, 651-673 (1977).
- Rosen, M. and M. Vazquez, "Secondary waves in Ribbing instability," *Nonequilibrium Statistical Mechanics and Nonlinear Physics, XV Conference. American Institute of Physics*, 14-19 (2007).
- Ruschak, K.J., "Coating Flows," *Ann. Rev. Fluid Mech.*, **17**, 65-89 (1985).
- Samways, N., "Hot Strip mill and coating facilities at the Middleton works," *Iron and Steel Eng.*, **4**, 15-22 (1989).
- Savage, M.D., "Mathematical models for coating processes," *J. Fluid Mech.*, **17**, 443-455 (1982).
- Varela López, F. and M. Rosen, "Rheological Effects in Roll Coating of Paints," *Latin American Applied Research*, **32**, 247-252 (2002).
- Varela Lopez, F., L. Pauchard, M. Rosen and M. Rabaul, "Non-Newtonian effects on Irving instability threshold," *J. Non-Newtonian Fluid Mech.*, **103**, 123-139 (2002).
- Varela Lopez, F., C. Correa, M. Vazquez and M. Rosen, "Experimental pressure distribution in roll coating flows: Newtonian and non Newtonian fluids," *Proceed. 5th European Coating Symposium*, 95-102 (2003).

Received: February 29, 2008

Accepted: June 24, 2008

Recommended by Subject Editor: Alberto Cuitiño